

MERCURY'S ROTATIONAL STATE FROM THE MERCURY LASER ALTIMETER. Erwan Mazarico¹, Michael K. Barker², Gregory A. Neumann¹, David E. Smith³, and Maria T. Zuber³. ¹Planetary Geodynamics Laboratory, NASA Goddard Space Flight Center, Greenbelt, MD 20771, USA (erwan.m.mazarico@nasa.gov); ²Sigma Space Corporation, Lanham, MD 20706, USA; ³Department of Earth, Atmospheric and Planetary Sciences, Massachusetts Institute of Technology, Cambridge, MA 02139, USA.

Introduction: From March 2011 to April 2015, the Mercury Laser Altimeter (MLA) instrument [1], onboard the MESSENGER spacecraft [2], collected over 22 million measurements of surface height with a vertical precision of ~ 1 m and accuracy of ~ 10 m. The MLA dataset contains ~ 3 million crossovers, instances where two ground-tracks intersect. These crossovers represent repeated measurements of the same surface locations and, thus, provide an opportunity to measure Mercury's orientation and rotation from close range [3]. Independent confirmation and refinement of the IAU libration model, developed from ground-based radar measurements [4], is important as it has implications for the moment of inertia of the outer solid shell and thus the mass distribution, internal structure and thermal evolution of Mercury. Here we describe the crossover dataset and the method used to recover the planet's rotational parameters. We model the relative vertical displacements between track pairs (crossover discrepancies) as the combined effect of errors in spacecraft (s/c) position and attitude reconstruction, and deviations from the IAU rotational model [4].

Instrument and Data Description: MESSENGER was in a highly elliptical, near-polar orbit around Mercury with a periaapsis of $\sim 200 - 400$ km, an apoapsis of $\sim 15,000$ km, and an orbital period of 12 hrs after orbit insertion (reduced to 8 hrs after one year). The spacecraft altitude was within ranging distance for 15 to 45 mins near periaapsis, typically at latitudes $>30^\circ$ N.

MLA was a time-of-flight laser altimeter operating at a wavelength of 1064 nm and with a firing rate of 8 Hz. Over the course of the mission, the transmitted laser pulse energy slowly declined due to expected degradation of the optics and the harsh thermal environment. It had 4 different output channels (0/1/2/4),

with different levels of precision and contamination from solar noise, with Ch. 0 having the highest precision and lowest noise, and Ch. 4 having the lowest precision and highest noise. In the course of the mission, the harsh thermal environment and related spacecraft constraints led to operation of MLA at slant angles as high as 70° .

The total MLA dataset contains $\sim 3,200$ tracks, ~ 22 million ranges, and ~ 3 million crossovers in the northern hemisphere (Fig. 2a). Because of the elliptical orbit, the laser spot size on the surface varied between $\sim 10 - 100$ m and the distance between each crossover and its bracketing points was usually <400 m.

Inversion Method: Prior to the crossover analysis, errors in the s/c position are reduced by fitting each MLA track to a polar stereographic topographic map covering latitudes $>55^\circ$ N. The resulting along-track, cross-track, and radial (ACR) adjustments to s/c position (Fig. 1a) improve the overall agreement between tracks (Fig. 1b) and are used as starting values next.

Each crossover is the intersection of two separate ground-tracks and, thus, represents two distinct measurements of the same surface location at two different times. Any difference in the height measurements at a crossover intersection is due largely to several effects: (1) Errors in the reconstructed s/c orbit, s/c attitude, MLA boresight orientation, (2) interpolation errors on the surface, and (3) geolocation errors due to mismodeled time-varying planetary rotational variations. We use the orbit reconstruction based on the HgM005 gravity field [5], and definitive project SPICE kernels.

We determined the best-fit rotational parameters through a weighted least-squares inversion of their partial derivatives and those of the along-track, cross-track, and radial offsets to s/c position, and roll and

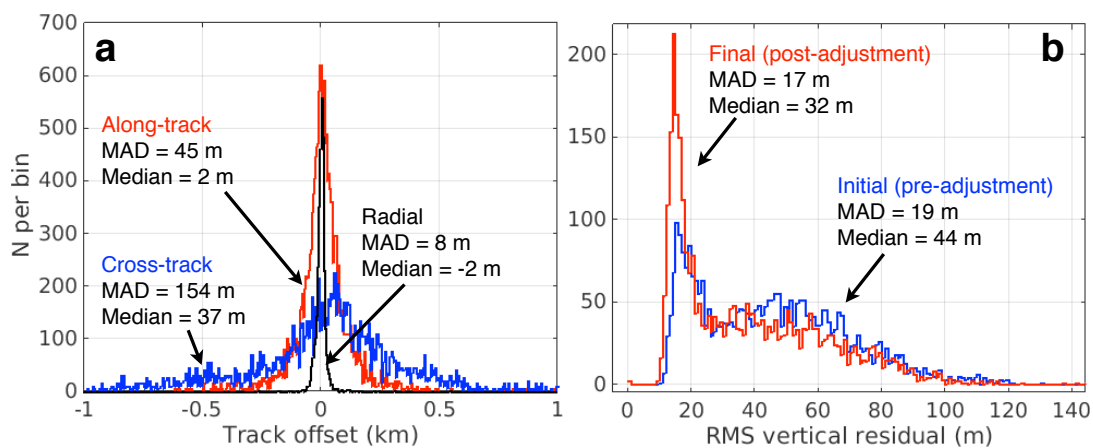


Figure 1. (a) Distribution of radial, cross-track and along-track *a priori* adjustments for each MLA track. Cross- and along-track are scaled by a factor of 5. (b) Distribution of RMS radial residuals before and after ACR adjustments to each track.

pitch offsets to *s/c* attitude. We chose 3 time bins per track, spaced to have roughly equal numbers of crossovers, yielding ~50,000 parameters total. There are four rotational parameters: right ascension and declination of the spin pole at J2000; rotation rate; amplitude of the libration. The quantity to be minimized is the total RMS crossover discrepancy with down-weighting of crossovers with abnormally large discrepancies. The spatial distribution of initial crossover discrepancies (Fig. 2b) resembles a map of surface roughness, implying that most of the remaining discrepancy is due to interpolation more than orbit/attitude errors.

The crossover partial derivatives of the libration amplitude tend to decrease in magnitude toward the north pole, a consequence of the constant longitudinal libration amplitude (~38.5'') causing a decreasing horizontal surface displacement closer to the pole. This suggests that it may be beneficial to assign higher weight to crossovers at lower latitudes.

For this work, we have used the 1.3 million highest-quality crossovers by excluding those with off-nadir angles >10° and inter-point distances >400 m. We neglect pointing errors to reduce the number of free parameters.

The parameter vector, *p*, is found by solving the normal equations:

$$p = (X^T W X + \lambda_2 M_2 + \lambda_A M_A + \lambda_C M_C + \lambda_R M_R)^{-1} (X^T W y)$$

where *X* is the design matrix of partial derivatives, *W* is the observation weight matrix, the λ 's are scalar weights on the constraint matrices, *M*, and *y* is the vector of crossover discrepancies. To reduce unphysical oscillations, constraints are placed on the offset magnitudes (*M_{A,C,R}*) and their 2nd derivative (*M₂*).

Preliminary results are shown in Figure 3.

Summary and Future Work: Mercury experiences perturbations which cause deviations from the 3:2 spin-orbit resonance, and physical longitudinal librations of ~450 m at the equator. The precise behavior depends on the planet's interior structure.

We have begun a project to harness the extensive

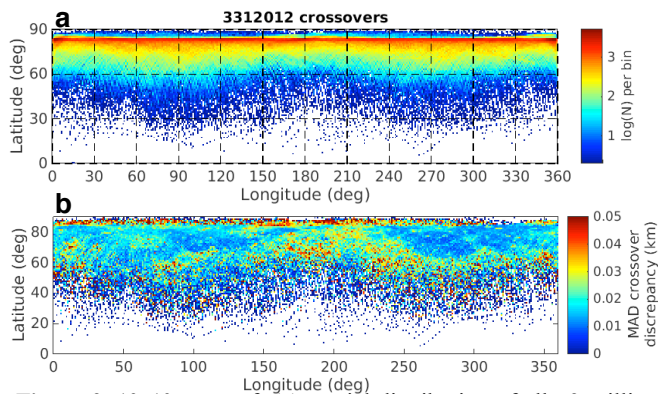


Figure 2. 1°x1° maps of: (a) spatial distribution of all ~3 million crossovers in the MLA dataset in 1°x1° bins; (b) median absolute deviation (MAD) of crossover discrepancies.

MLA altimetric dataset of ground-track crossovers to measure deviations of the planet's rotation from the IAU model. Careful consideration of the *s/c* orbital errors and MLA pointing biases will allow estimating libration amplitude, pole position, and mean spin rate.

To fully characterize the behavior of the solutions, we are conducting simulations with times-of-flight generated self-consistently from realistic topography. This will allow a better understanding of the sensitivities of the rotational parameters to the weights on the crossovers and the constraints. We will employ variance component estimation to fit the data with the optimal weights on the constraints, and to perform a full covariance analysis of all parameters. The solution accuracy will also be improved by iteratively re-calculating the partial derivatives. A longer time baseline may be achieved by incorporating crossovers from the two MESSENGER flybys of Mercury in 2008.

References: [1] Cavanaugh J.F. *et al.* (2007), *Space Sci. Rev.* 131, 451-480. [2] Solomon S.C. *et al.* (2007), *Space Sci. Rev.* 131, 3-39. [3] Stark A. *et al.* (2015), *Geo. Phys. Rev. Let.* 42, 788. [4] Margot J.-L. (2009), *Celest. Mech. Dyn. Astron.* 105, 329-336. [5] Mazarico E. *et al.* (2014), *JGR Planets*, 2417-2436.

We acknowledge support of NNH13ZDA001N-PGG.

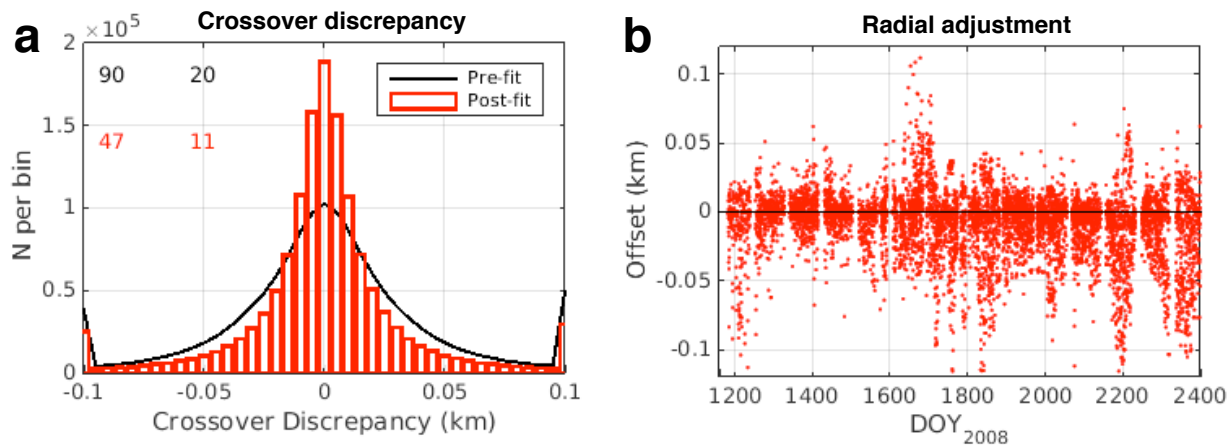


Figure 3. Initial results of inversion after one iteration. (a) Histogram of pre-fit (black) and post-fit (red) crossover discrepancies. (b) Best-fit radial offsets vs. time.